Available online at www.sciencedirect.com
SCIENCE DIRECT®
Solid State Communications 129 (2004) 491–495
solid state communications
www.elsevier.com/locate/ssc

A spectroscopic ellipsometry study on the variation of the optical constants of tin-doped indium oxide thin films during crystallization

Yeon Sik Jung*

Research and Development Center, Samsung Corning, 644, Jinpyoung-dong, Gumi, Kyoung-buk 730-725, South Korea

Received 14 August 2003; received in revised form 29 October 2003; accepted 30 November 2003 by H. Akai

Abstract

In this paper, the variation of the optical constants of tin-doped indium oxide thin films during thermal treatment was explored using spectroscopic ellipsometry based on appropriate analysis models combining a Drude absorption edge and Lorentz oscillators. It was found that the refractive indices and the extinction coefficients show different behaviors depending on depth, thermal treatment time and temperature. The optical constants varied more abruptly in the lower part of the films, which confirms the model that crystallization starts from the film-substrate interface. Hall measurement showed that the significant increase in the extinction coefficients in the near infrared range is due to the increased number of free electrons.
© 2003 Elsevier Ltd. All rights reserved.

PACS: 78.20.Ci

Keywords: A. Thin films; D. Optical properties; E. Light absorption and reflection

1. Introductions

Tin-doped indium oxide (ITO) thin films have been commonly used as transparent conducting films for opto-electronic applications due to low resistivity, high transmittance, and good etching properties [1–3].

The use of spectroscopic ellipsometry (SE) for measuring the optical constants (refractive index and extinction coefficient) of ITO thin films has been reported by many researchers [4–10]. In addition, in situ or ex situ monitoring of film crystallizations by ellipsometry have been presented [8,11–14]. Plots of measured tan Ψ (the amplitude ratio of the reflection coefficients of p- and s-polarized lights) and cos Δ (the phase difference between the two polarized lights) values against annealing time show typical S-shaped transformation curves [13]. In addition, SE has the advantages of requiring a short measurement time (about 10 min) and being non-destructive. Thus, SE could be an effective and convenient method for monitoring the crystallization of materials.

ITO thin films have highly graded structures through the film depth, and the gradient makes it difficult to get a good agreement between their measured and calculated Ψ and Δ spectra with a simple one-layer model [5,7–9]. Thus, several ways to describe the graded structure have been proposed. One is to assume a linear grade of the optical constants through the film depth using the effective medium approximation (EMA) [6,7,15]. However, in the cases of strong gradient or thicker film thickness than several tens of nanometers, it was generally recommended to split the film into multiple uniform films and to conduct model-fitting the optical constants of each film [16].

In this paper, the change of optical constants of sputter-deposited ITO thin film during thermal treatment was monitored and analyzed by using spectroscopic ellipsometry with appropriate analysis models. It was found that the

* Present address: Korea Institute of Science and Technology, Thin Films Research Center, 39-1 Hawolgok-dong, Seongbuk-gu, Seoul 136-791, South Korea. Tel.: +82-2-958-5565; fax: +82-2-958-6851.

E-mail address: ysjung@kist.re.kr (Y.S. Jung).

0038-1098/$ - see front matter © 2003 Elsevier Ltd. All rights reserved.
doi:10.1016/j.ssc.2003.11.044

refractive indices and the extinction coefficients vary significantly as functions of depth, thermal treatment time and temperature, which confirms the previously proposed crystallization models of ITO thin films. Hall effect measurement was also carried out to support the analyses.

2. Experimental

2.1. Preparation of samples

ITO thin films were sputter-deposited using an ITO target in an in-line magnetron sputter-deposition system equipped with DC power. The chamber, which was equipped with a load-lock system and diffusion pumps, had a base pressure of 6×10^{-4} Pa. The target (128 mm × 450 mm) used was a sintered ITO containing 10 wt% SnO_2 (99.99%). Sputtering was carried out at a pressure of 0.1 Pa in pure Ar gas. The samples were deposited without heating the substrates. The films were deposited on p-type (100) Si wafers, which were placed 50 mm apart and parallel from to target surface. The wafers were cleaned in an ultrasonic bath containing a detergent at 65 °C for 6 min, and then rinsed in deionized water in the ultrasonic bath for another 15 min. The cleaned substrates were dried at 100 °C for 15 min. The target was pre-sputtered for 3 min. The thickness of the films was about 300 nm. The thermal treatment was performed by varying the time from 3 to 120 min, and maintaining the temperature at 200 and 300 °C. The treatment was carried out under vacuum (1×10^{-3} Pa) to avoid undesirable incorporation of reactive gases.

2.2. Data analysis

Ψ and Δ spectra were acquired using a spectroscopic ellipsometer (J.A. Woollam Co., VASE®) [4,7]. The measurement was conducted in the spectral range of 300–1200 nm at three angles of incidence (65, 70, and 75°) in steps of 10 nm. The analysis of optical constants was based on the model shown in Fig. 1. An SiO_2 interfacial layer with the thickness of 4 nm was inserted in the model to improve the quality of fit. The optical constants of the ITO layers were analyzed based on a model combining a Drude absorption edge and Lorentz oscillators. To analyze the graded structure of the films, two independent layers were used for the fitting model. The fit result was reproducible, and the quality of fit, which was estimated by the mean square deviation, was much better than in the case of a one-layer model. With a three-layer model, the obtained optical constants were unphysical and not reproducible, and the fit parameters were significantly correlated with each other. As other researchers have suggested, fitting only a minimum number of parameters typically weakens the correlation [7]. The three-layer model requires too many fit parameters, and thus it was thought to be inappropriate. The same thickness was used for the lower and the upper layers, which was about 150 nm. No considerable change in thickness was observed after thermal treatment. The surface roughness layer was modeled with the Bruggeman effective medium approximation (BEMA), where a mixture of 50% top ITO film and 50% voids are assumed [8,9]. The thickness of the BEMA layer was also selected as a fit parameter. From a Lorentz oscillator model, the complex dielectric function can be expressed as follows [7,12]:

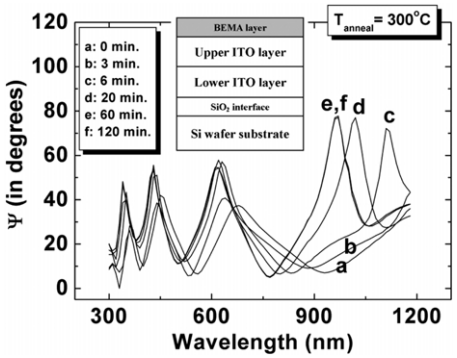

Fig. 1. Four-layer model for analyzing SE data, and measured Ψ—curves of the ITO sample annealed at 300 °C with different annealing time.

$$\varepsilon(E) = \varepsilon(\infty) + \sum_{i=1}^{N} \frac{A_i}{E_i^2 - E^2 - \mathrm{i}\Gamma_i E} \tag{1}$$

where $\varepsilon(E)$ is the complex dielectric function as a function of photon energy, E, $\varepsilon(\infty)$ is the dielectric function at infinite energy, A_i is the amplitude, Γ_i is the broadening, and E_i is the center energy of the ith oscillator, respectively [7,16]. The four terms ($\varepsilon(\infty)$, A_i, Γ_i, and E_i) were used as fit parameters. The center energy of the first oscillator was fixed at 0 to describe free carriers based on the Drude model.

The concentration and the mobility of electrons were measured using Hall effect and Van der Pauw's technique with magnetic field of 0.320 T, and the data were measured 10 times and averaged to reduce the effects of random noises.

3. Results and discussions

Fig. 1 shows the curves of the measured Ψ against wavelength for different thermal treatment times. The samples were thermally treated at 300 °C. The curves shifted towards the direction of shorter wavelength. The curves of the samples annealed for 60 and 120 min almost overlapped each other, which means the saturation of optical constants has occurred at or before a 60 min thermal treatment time. Thus, the amount of crystallization can be calculated by monitoring the change of Ψ or Δ values [13].

The refractive indices and optical constants, which were

obtained from the layer stacking model shown in Fig. 1 and the measured Ψ and Δ curves as functions of wavelength, are presented in Fig. 2(a) and (b). The optical constants were extracted from the upper layer in the model. The refractive indices decreased with increasing thermal treatment time. The decrease of refractive indices after annealing ITO films was reported [5]. Some researchers have reported that the indices of refraction of SiO_2 or TiO_2 thin films decrease after heat treatment [17,18]. H. Poelman et al. has proposed that the decrease of refractive indices is due to lower packing densities, resulting from the microstructural changes in the layer by thermal treatment [17]. H.Z. Massoud et al. also found that the refractive index of SiO_2 thin film increased with compressive stress and explained that the decrease of refractive index during heat treatment is due to stress relaxation [18]. These arguments would suggest that generated voids due to the growth of crystallites during thermal treatment may be responsible for the decrease of refractive indices. The refractive indices of the samples annealed for 60 and 120 min were the same, which again shows the saturation of optical constants has occurred at or before a 60 min. thermal treatment.

Fig. 2(b) shows the variation of extinction coefficients against wavelength for different thermal treatment times. The origin of high extinction coefficients in the near infrared region, which is known as Drude edge, is the interaction of light with the free carriers in ITO films since the plasma frequency of ITO films is about 750–800 nm [9]. In the visible range, higher extinction coefficients can be originated from sub-oxide phases such as InO_x or SnO_x or crystallographic flaws (for example, grain boundaries and voids). The non-stoichiometric sub-oxide phases act as optical scattering centers [19]. The sub-oxide phases are expected to be formed due to oxygen deficiency or low crystallinity. In addition, higher absorption in the infrared can result in higher absorption in the visible range due to the long tail of the Lorentzian functions [7]. The extinction coefficients in the infrared range increases with the thermal treatment time, which may be due to the increase of free carriers. It is reported that the solubility of Sn increased as the deposition temperature of ITO increased [20], which means sufficient activation energy is essential for the n-type doping of Sn atoms. More Sn atoms in substitutional sites would produce more free electrons. The decrease of extinction coefficients in the visible range for the sample annealed for 6 min may be due to the reduction of crystallographic flaws. The extinction coefficients in the range increased again for the samples treated for more than

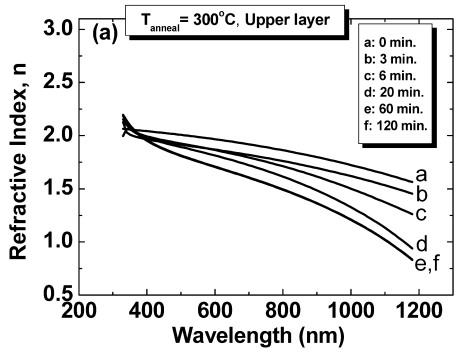

Fig. 2. Variation of (a) refractive indices and (b) extinction coefficients of the ITO films annealed at 300 °C with different annealing times.

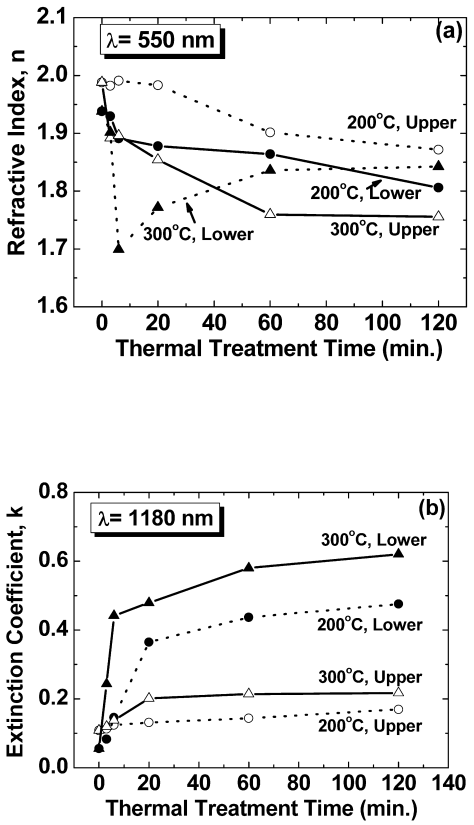

Fig. 3. Variation of (a) refractive indices and (b) extinction coefficients of the ITO films depending on the depths, different annealing times, and temperatures.

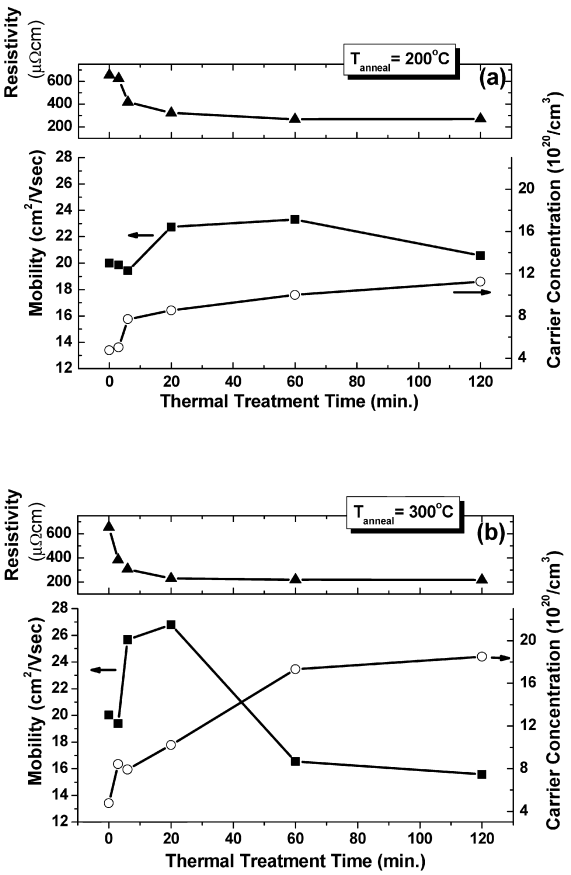

Fig. 4. Hall measurement results of the ITO samples with increasing thermal treatment time, for the treatment temperatures of (a) 200 °C and (b) 300 °C.

20 min, which may be due to the influence of the abrupt increase of absorption in the infrared range.

Fig. 3(a) shows the change of refractive indices at 550 nm for different thermal treatment times, temperatures, and the film depths. The refractive indices of oxide materials are proportional to film density [21,22]. Thus, monitoring the change of refractive index could be an indirect measure of film density. We assumed two independent layers in the analysis model shown in Fig. 1 to explore the variation of the optical constants depending on the depth in the ITO films. For the ITO samples annealed at 200 °C, the refractive index continuously decreased with time. The graphs did not show any saturation behavior until 120 min. The refractive index of the upper and lower layer decreased 5.5 and 6.7% after 120 min, respectively. The decrease in the case of the lower layer during the initial 20 min was 3.3%, while the refractive indices of the upper layer hardly changed during the same annealing time. From these results, it can be concluded that the movement of atoms and crystallization starts from the bottom of the films. This result confirms the crystallization model of ITO thin films proposed by H. Morikawa et al. [23]. Morikawa suggested that as-deposited ITO films at room temperatures have a certain amount of fine crystals at the interface with the substrate, and the crystals at the interface grow larger by heat-treatment [23]. This can be another example that SE can be used for exploring the crystallization mechanism non-destructively and effectively. The refractive indices for the ITO samples annealed at 300 °C show a much more drastic change. The refractive indices in the lower layer abruptly decreased during the first 6 min, and then increased until 60 min. The decrease during the first 6 min was about 15%. Due to the rapid crystallization, many voids would form in the lower part of the sample. The increase in refractive indices after 6 min means that densification occurred in the lower part of the films. While the increase of the refractive indices in the lower layer occurred from 6 to 60 min, the refractive indices in the upper layer significantly decreased. Then, the densification is thought to arise because of the diffusion of atoms from the upper layer to the voids in the lower layer. On the other hand, there was no sign of densification in the lower layer annealed at 200 °C until 120 min. It was reported that the crystallization of ITO thin films requires the temperature to be over 180–190 °C [24]. The temperature of 200 °C may be slightly higher than the lowest temperature for the crystallization of ITO films. Thus, the supplied activation energy and the crystallization speed at 200 °C would be much lower than those of the samples annealed at 300 °C. The refractive indices in the upper layer annealed at 300 °C decreased until 60 min, and then showed a saturation behavior. The amount of decrease was about 11%, which is about twice as much as the change at 200 °C.

Fig. 3(b) presents the change of extinction coefficients at 1180 nm for different thermal treatment times, temperatures, and the film depths. The increase in the extinction coefficients was larger for higher temperatures, longer treatment times, and the lower part of the ITO samples. Fig. 4(a) and (b) shows the Hall measurement result of the ITO samples. The free electron concentration was much higher for the samples treated at higher temperatures and during longer treatment times. These provide clear evidence that the significant increase in the extinction coefficients in the near infrared range is due to the increased number of free electrons. Higher extinction coefficients for the lower layers annealed at each temperature may be due to more active crystallization of the part, which is in agreement with the considerable change in refractive indices of the layers shown in Fig. 3(a).

The main factors affecting the Hall mobility of ITO thin films are the scattering at the grain boundary, the ionized impurities, and the film surface [25–27]. The change of carrier mobility shown in Fig. 4(a) and (b) can be divided into three steps. At the first stage, the Hall mobility decreased, which may be the result of the formation of new grain boundaries [27]. Grain growth and improved crystallinity may sharply increase the electron mobility in

the films at the second step. At the third step, the effect of the increased number of ionized donors such as oxygen vacancies or Sn^{+4} ions, which are the sources of free electron carriers, may overwhelm the improvement of crystallinity. In spite of a significant increase of carrier concentration, the resistivity hardly increased due to the decrease of mobility at the third step. This variation of mobility was similar between the samples annealed at different temperatures, except that the change occurred more rapidly at 300 °C.

4. Summary

Crystallization behavior of ITO thin films was studied by spectroscopic ellipsometry. Using the measured Ψ and Δ data, and appropriate analysis models combining a Drude absorption edge and Lorentz oscillators, optical constants of ITO samples with different depths, thermal treatment times and temperatures were obtained. The refractive indices largely decreased with thermal treatment, which may be due to the generated voids resulting from the growth of crystallites. The refractive indices and extinction coefficients changed more abruptly for the lower part of the films, and this confirms the model that crystallization starts from the film-substrate interface. In addition, the significant increase in the extinction coefficients in the near infrared range was explained from the increased number of free electrons quantified by Hall effect measurement.

References

[1] G. Haacke, Annu. Rev. Mater. Sci. 7 (1977) 73.
[2] C.G. Granqvist, Appl. Phys. A 52 (1991) 83.
[3] A.K. Kulkarni, K.H. Schulz, T.S. Lim, M. Khan, Thin Solid Films 345 (1999) 273.
[4] J.A. Woolam, W.A. McGahan, B. Hohs, Thin Solid Films 241 (1994) 44.
[5] J.N. Hilfiker, R.A. Synowicki, J.S. Hale, C. Bungay, Society of Information Display, Digest of Technical Papers, San Diego, 2002, p. 491.
[6] H.E. Rhaleb, E. Benamar, M. Rami, J.P. Roger, A. Hakam, A. Ennaoui, Appl. Surf. Sci. 201 (2002) 138.
[7] R.A. Synowicki, Thin Solid Films 313–314 (1998) 394.
[8] M. Losurdo, D. Barreca, P. Capezzuto, G. Bruno, E. Tondello, Surf. Coat. Technol. 151–152 (2002) 2.
[9] M. Losurdo, M. Giangregorio, P. Capezzuto, G. Bruno, R.D. Rosa, F. Roca, C. Summonte, J. Pia, R. Rizzoli, J. Vac. Sci. Technol., A 20 (2002) 37.
[10] L.J. Meng, E. Crossan, A. Voronov, F. Placido, Thin Solid Films 422 (2002) 80.
[11] A. Hultaker, K. Jarrendahl, J. Lu, C. Granqvist, G.A. Niklasson, Thin Solid Films 392 (2001) 305.
[12] C.H. Kuo, I.C. Hsieh, D.K. Schroder, G.N. Maracas, S. Chen, T.W. Sigmon, Appl. Phys. Lett. 71 (1997) 359.
[13] H. Seo, T.H. Jeong, J.W. Park, C. Yeon, S.J. Kim, S.Y. Kim, Jpn. J. Appl. Phys. 39 (2000) 745.
[14] P. Petrik, C. Schneider, Vacuum 61 (2001) 427.
[15] D.A.G. Bruggeman, Ann. Phys. 24 (1935) 636.
[16] J.A. Woollam Co., Guide to Using WVASE32™. p. 329.
[17] H.Z. Massoud, H.M. Przewlocki, J. Appl. Phys. 92 (2002) 2202.
[18] H. Poelman, D. Poelman, D. Depla, H. Tomaszewski, L. Fiermans, R. De Gryse, Surf. Sci. 482–485 (2001) 940.
[19] Y. Shigesato, D.C. Paine, E. Haynes, Jpn. J. Appl. Phys. 32 (1993) L1352.
[20] F. El Akkad, M. Marafi, A. Punnoose, G. Prabu, Phys. Status Solidi A 177 (2000) 445.
[21] J. Szczyrbowski, G. Brauer, M. Ruske, J. Bartella, J. Schroeder, A. Zmelty, Surf. Coat. Technol. 112 (1999) 261.
[22] B. Hunsche, M. Vergohl, H. Neuhauser, F. Klose, B. Szyszka, T. Matthee, Thin Solid Films 392 (2001) 184.
[23] H. Morikawa, H. Sumi, M. Kohyama, Thin Solid Films 281–282 (1996) 202.
[24] P.K. Song, H. Akao, M. Kamel, Y. Shigesato, I. Yasui, Jpn. J. Appl. Phys. 38 (1999) 5224.
[25] D. Mergel, M. Schenkel, M. Ghebre, M. Sulkowski, Thin Solid Films 392 (2001) 91.
[26] H. Klauk, J. Huang, J.A. Nichols, T.N. Jackson, Thin Solid Films 366 (2000) 272.
[27] H. Morikawa, M. Fujita, Thin Solid Films 339 (1999) 309.